NUMERICAL MODELLING OF FIBRE METAL LAMINATES UNDER THERMO-MECHANICAL LOADINGS

M. Hagenbeek[1*], S.R. Turteltaub[2]
[1] INHolland Composites Lab, INHolland University of Applied Sciences, Delft, The Netherlands, [2] Koiter Institute Delft, Delft University of Technology, Delft, The Netherlands
* Corresponding author (michiel.hagenbeek@inholland.nl)

Keywords: *thermo-mechanical behaviour, solid-like shell element, fibre metal laminates*

1 General Introduction

A thermo-mechanical finite element model, based on a solid-like shell element, has been developed. The use of standard continuum elements to model thin-walled structures, such as a fuselage skin, may lead to problems as they tend to show Poisson-thickness locking for high aspect ratios.

Therefore a solid-like shell element has been extended to include the temperature field and thermal expansion. The coupled system of equations is solved simultaneously. This numerical model is used to characterise the behaviour of fibre metal laminates under thermo-mechanical loadings.

A bi-material strip subjected to a heat source is presented as a benchmark test to demonstrate the performance of the thermo-mechanical solid-like shell element. With a minimum amount of elements and a high aspect ratio the results are accurate and in agreement with the analytical solution.

2 The development of fibre metal laminates

The development of fibre metal laminates resulted in an improved fatigue performance and higher residual strength [1, 2]. However, the use of different constituents also raises new questions especially regarding the thermo-mechanical properties. Differences in thermal expansion coefficients cause residual stresses after curing of the laminate. And in service, when the temperature can vary between -55 up to 70°C due to solar radiation and convection, internal stresses can be expected as well. For asymmetric lay-ups this will lead to secondary bending.

On the other hand, the combination of constituents appears to possess unexpectedly good thermal insulation [3]. This property leads to a relative low temperature on the inside of Glare panels in burn-through tests [4]. Moreover, the final burn-through time increases significantly and therefore the application of Glare in the fuselage skin means a major improvement in aircraft safety.

3 Numerical modelling with the solid-like shell

Finite element simulations can be of assistance to investigate thin-walled Glare structures under thermo-mechanical loading. In the present paper the development of a mesoscopic model is discussed.

The uncoupled thermo-mechanical 3D-analysis process of composite structures was shown by Rolfes et al [5], where a shell finite element model was used throughout. The mechanical part in their research consists of thermally induced stresses, which are also calculated in transverse direction [6]. The use of standard continuum elements to model thin-walled structures, as the fuselage skin, may lead to problems. They tend to show Poisson-thickness locking when their aspect ratios (i.e. the ratio of element length over its width) are too high. As a result, the elements become overly stiff.

An alternative method discussed in this paper is the so-called solid-like shell element, which can describe the behaviour of fibre metal laminates in a fully three-dimensional state [7, 8] and which can handle failure mechanisms like cracking and delamination in connection with interface elements as shown by Remmers et al [9].

The 8 or 16 external nodes have three degrees of freedom in the case of only mechanical loading, since only the displacements are considered. For the thermo-mechanical solid-like shell element a temperature field and thermal expansion is included. Consequently, each external node has four degrees of freedom, the three displacements, $\hat{u}_x$, $\hat{u}_y$, and $\hat{u}_z$, and the temperature at the node $\hat{\theta}$.

By adding the temperature degree of freedom only at the corner nodes of the sixteen-node element eventual numerical instability, due to a

difference in order for mechanical and thermal strain, can be avoided. The coupled system of equations is solved simultaneously.

4. Constitutive relations

The stress tensor consists of a mechanical induced part and a thermal expansion part. The mechanical stress tensor can be written as the relation between the second Piola-Kirchhoff stress and the Green-Lagrange strain tensor $\boldsymbol{\gamma}^{GL}$. The thermal stress tensor is written in a similar way with the thermal strain tensor $\boldsymbol{\gamma}^{\alpha}$. Thus:

$$\boldsymbol{\sigma} = \boldsymbol{D}^{GL}\boldsymbol{\gamma}^{GL} - \boldsymbol{D}^{\alpha}\boldsymbol{\gamma}^{\alpha}, \tag{1}$$

where $\boldsymbol{D}^{GL}$ is the tangent stiffness matrix for the Green-Lagrange strains and $\boldsymbol{D}^{\alpha}$ is the thermal expansion matrix, which consists of the thermal expansion coefficients times the bulk modulus:

$$\boldsymbol{D}^{\alpha} = \begin{bmatrix} \alpha_1 D_{11} & 0 & 0 & 0 & 0 & 0 \\ 0 & \alpha_2 D_{22} & 0 & 0 & 0 & 0 \\ 0 & 0 & \alpha_3 D_{33} & 0 & 0 & 0 \\ 0 & 0 & 0 & 0 & 0 & 0 \\ 0 & 0 & 0 & 0 & 0 & 0 \\ 0 & 0 & 0 & 0 & 0 & 0 \end{bmatrix}, \tag{2}$$

The Green-Lagrange strain tensor is conventionally written in terms of the deformation gradient $\boldsymbol{F}$:

$$\boldsymbol{\gamma}^{GL} = \frac{1}{2}(\boldsymbol{F}^{T}\boldsymbol{F} - \boldsymbol{I}). \tag{3}$$

The deformation gradient $\boldsymbol{F}$ can be written as a function of the covariant base vector in the deformed configuration $\boldsymbol{g}_i$ and the contravariant base vector in the undeformed reference configuration $\boldsymbol{G}_i$. This lead to the following expression for the mechanical strain tensor $\boldsymbol{\gamma}^{GL}$:

$$\boldsymbol{\gamma}^{GL} = \gamma_{ij}^{GL}\boldsymbol{G}^{i} \otimes \boldsymbol{G}^{j}; \tag{4}$$

where

$$\gamma_{ij}^{GL} = \frac{1}{2}(g_{ij} - G_{ij}). \tag{5}$$

Similarly, the thermal expansion strain tensor $\boldsymbol{\gamma}^{\alpha}$ can be written as:

$$\boldsymbol{\gamma}^{\alpha} = \gamma_{ij}^{\alpha}\boldsymbol{G}^{i} \otimes \boldsymbol{G}^{j}; \tag{6}$$

where

$$\gamma_{ij}^{\alpha} = \theta\, G_{ij}, \tag{7}$$

and θ is the relative temperature. The thermal expansion in composites is in general orthotropic; the expansion is different in fibre direction and transverse to the fibre direction.

The thermal strain tensor $\delta\boldsymbol{\gamma}_{ij}^{\alpha}$ is a function of the virtual temperature field in the element and will be derived similar to the derivation of the virtual Green tensor $\delta\boldsymbol{\gamma}_{ij}^{GL}$ as function of the virtual displacement $\delta\hat{\boldsymbol{u}}$ as performed by Hashagen [8]. The thermal expansion provides the coupling between the temperature field and the displacement field. Vice versa, strong deformations could cause thermal heat in the structure. However in the current derivation this effect is not considered as it plays a minor role in an aircraft structure.

For the 16 node element only at the 8 corner nodes the temperature is included. For the displacement field second-order shape functions are thus used and for the temperature field first-order functions. In this way both the mechanical strain, due to mechanical loading, and the thermal strain, due to expansion, are of the same order. The mechanical strain follows from the displacement variation and the thermal strain follows directly from the temperature distribution times the thermal expansion coefficient in a given direction. Hence, both the displacements due to mechanical loading and due to thermal loading have a constant distribution over the element. Same order shape functions for the temperature and displacement field can lead to slightly different values at the integration points within one element, and causes a so called "checkerboard" pattern in the calculation field which

can lead to a non-convergent solution. With the different order in shape functions this problem is avoided.

The effect of a certain heat source on the temperature distribution is calculated with the heat transfer equations from the first law of thermodynamics:

$$\rho C_p \dot{\theta} + K_\theta \theta = Q\,, \tag{8}$$

where ρ is the mass density, C_p is the specific heat, θ is the temperature relative to the outside temperature, K_θ is the thermal conductivity, and Q is the external heat flow input. Initially the time-dependency and material non-linearities are left out of the consideration. The heat transfer equation reduces to the following steady state model:

$$K_\theta \theta = Q\,. \tag{9}$$

Or written with the principle of virtual temperatures:

$$\int_V \dot{\boldsymbol{\theta}}^T \mathrm{k}\, \dot{\boldsymbol{\theta}}\, dV = \boldsymbol{Q} \tag{10}$$

where $\dot{\boldsymbol{\theta}}^T$ is defined as

$$\dot{\boldsymbol{\theta}}^T = \begin{bmatrix} \theta_{,x} \\ \theta_{,y} \\ \theta_{,z} \end{bmatrix}, \tag{11}$$

and the thermal conductivity matrix $\boldsymbol{k}$ in case of an orthotropic material is:

$$\boldsymbol{k} = \begin{bmatrix} k_{xx} & & \\ & k_{yy} & \\ & & k_{zz} \end{bmatrix}. \tag{12}$$

The matrix formulation of the complete steady state thermo mechanical model in general form for the solid like shell element can be presented as:

$$\begin{bmatrix} \boldsymbol{K}_u & \boldsymbol{K}_\alpha \\ \boldsymbol{K}_\alpha^T & \boldsymbol{K}_\theta \end{bmatrix} \begin{bmatrix} \hat{\boldsymbol{u}} \\ \hat{\boldsymbol{\theta}} \end{bmatrix} = \begin{bmatrix} \boldsymbol{F} \\ \boldsymbol{Q} \end{bmatrix}. \tag{13}$$

In the finite element implementation the equations are linearised and solved in a Newton-Raphson process. The internal degrees of freedom, which are used to add a quadratic term to the displacement field in the thickness direction, are not able to support an external loading and are eliminated on element level by condensation as suggested by Parisch [7].

3 Bi-material strip subjected to a heat source

To illustrate the application and performance of the new solid-like shell element a bi-material strip is considered, where two strips with different thermal expansion coefficient are bonded together, see Figure 2.

The analysis is performed with an eight-node element. The aspect ratio S = *l*/*h* is high, S = 100. The strip is kept at a constant temperature θ of 2.5 °C. An aluminium 2024-T3 strip of 0.3 mm on top of a glass-fibre epoxy layer of 0.127 mm will be considered here, with the fibre orientation in the length of the strip. The material property data of the glass-fibre epoxy have been derived by testing [10].

The other dimensions are 300 mm for the length *l*, and 30 mm for the width *w*. Two times 10 elements are used to model both strips numerically. The numerical simulation is found to be in good agreement with the analytical solution [11]. The results are shown in Figure 3.

4 Results and discussion

The constituents of fibre metal laminates show differences in thermal expansion which lead to residual stresses and, in case of asymmetric lay-up, to secondary bending.

To understand and calculate the effect of temperature on the material the solid-like shell element developed in earlier research is extended to include thermal expansion and heat transfer. With the thermo-mechanical solid-like shell element finite element simulations can be performed to investigate the thermal effects for Glare in detail. The simulation will be used to analyse the material behaviour for in-service temperature conditions (-55 up to 70 °C).

Benchmark tests (performed for aluminium 2024-T3 and glass-fibre epoxy) show the good agreement between analytically and numerically determined elongation and deflection of a long, thin bi-material strip with high aspect ratio.

References

[1] L. Vogelesang, J. Schijve, and R. Fredell "Fibre-metal laminates: damage tolerant aerospace materials". *Case Studies in Manufacturing with Advanced Materials,* Vol. 2, pp 253-271, 1995.

[2] R. Alderliesten, Fatigue, in: A. Vlot, J. W. Gunnink (Eds.) "*Fibre Metal Laminates an Introduction"*. 1st edition, Kluwer Academic Publishers, Dordrecht, The Netherlands, pp 155-171, 2001.

[3] G. Roebroeks "Glare, a structural material for fire resistant aircraft fuselages". *Proceedings of Conference AGARD*, Dresden, Vol. 587, paper number, pp 26/1-26/13, 1997.

[4] P. Hooijmeijer, and P. Kuijpers "*Fire testing and properties of Glare material: A literature survey"*, Tech. Rep. B2v-99-25, GTO sub-project 5.1.2.1, Delft University of Technology, 1999.

[5] R. Rolfes, J. Noack, and M. Taeschner "High performance 3D-analysis of thermomechanically loaded composite structures", *Composite Structures*, Vol. 46, pp 367-379, 1999.

[6] R. Rolfes, J. Tessmer, and K. Rohwer "Models and tools for heat transfer, thermal stresses and stability of composite aerospace structures", *Journal of Thermal Stresses*, Vol. 26, No. 6, pp 641-670, 2003.

[7] H. Parisch, "A continuum-based shell theory for non-linear applications", *International Journal for Numerical Methods in Engineering 38* (11), pp 1855-1833, 1995

[8] F. Hashagen, "Numerical Analysis of Failure Mechanisms in Fibre Metal Laminates", Ph. D. thesis., Delft University of Technology, Delft, 1998

[9] J. Remmers, R. de Borst, "Numerical modelling: Delamination buckling", in A. Vlot, J.W. Gunnink (Eds.), Fibre Metal Laminates an Introduction, Kluwer Academic Publishers, Dordrecht, The Netherlands, pp. 281-297, 2001.

[10] M. Hagenbeek "*Characterisation of Fibre Metal Laminates under thermomechanical loadings"*. Ph.D. thesis, Delft University of Technology, Delft, The Netherlands, 2005.

[11] T. Clyne "Residual stresses in surface coatings and their effects on interfacial debonding", *Key Engineering Materials*, Vol. 116, No. 7, pp 307-330, 1996.

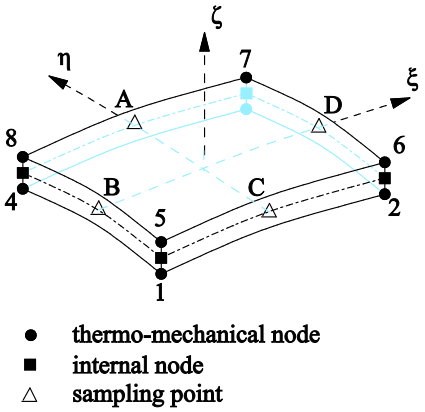

Fig. 1. Geometry and location of the sampling points A-D of the eight-noded thermo-mechanical solid-like shell element.

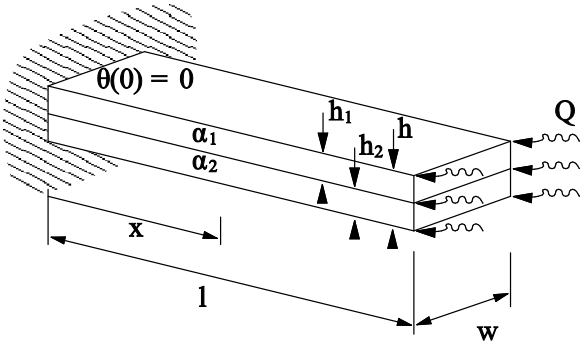

Fig. 2. Benchmark test for the solid-like-shell element: a bi-material strip subjected to a heat source.

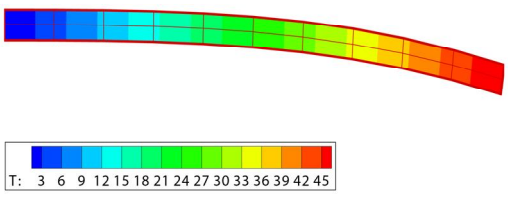

Fig. 3. Deflection and temperature distribution of the bi-material strip subjected to a heat source.